JOURNAL OF SOLID STATE CHEMISTRY **127,** 82–86 (1996)
ARTICLE NO. 0359

A TEM and Powder XRD Study of New Fluorite and Perovskite-Related Phases in the $CaO–ZrO_2–Ta_2O_5$ System

Siegbert Schmid, Charlene Lobo, Ray L. Withers,[1] and John G. Thompson

Research School of Chemistry, Australian National University, Canberra, ACT 0200, Australia

Received May 13, 1996; accepted August 14, 1996

A new long period, anion-deficient, fluorite-related superstructure phase ($a = 36.372(3)$, $b = 7.3590(5)$, and $c = 31.018(8)$ Å) has been discovered in the $CaO–ZrO_2–Ta_2O_5$ system at an experimentally determined composition of $0.304(4)TaO_{2.5} \cdot 0.347(4)ZrO_2 \cdot 0.349(4)/CaO$. Electron diffraction suggests a space group symmetry for this phase of *Fddd*. It is furthermore shown that substantial amounts of Ta_2O_5 can be incorporated into $CaZrO_3$ without apparently altering structure type. Extremely sluggish kinetics, however, make it difficult to determine the extent of this perovskite-related solid solution. © 1996 Academic Press, Inc.

1. INTRODUCTION

Neurgaonkar *et al.* (1) first reported the existence of an unidentified new phase in the $LiTaO_3–CaZrO_3$ system over the whole of the composition range from 21 to 70 mol% $CaZrO_3$. They also reported the existence of a two phase region from 70 to 95 mol% $CaZrO_3$ separating this new phase from an orthorhombic perovskite type, $CaZrO_3$ solid solution phase. Subsequently, Smith and West (2) reinvestigated the $LiTaO_3–CaZrO_3$ system and confirmed the existence of both the new phase (from 27 to 88 mol% $CaZrO_3$) and the two phase region (from 88 to 95 mol% $CaZrO_3$) separating it from the $CaZrO_3$ solid solution phase. It was furthermore shown, via Rietveld structure refinement, that Neurgaonkar *et al.*'s new phase and the $CaZrO_3$ solid solution phase were extremely closely related, both in terms of unit cell dimensions and space group symmetry, as well as in terms of fractional coordinates. The exact cause of the immiscibility gap separating these two orthorhombic perovskite type phases, however, was not identified.

The present paper had its genesis in an attempt to understand the structural origin of the reported two phase region. Following the same experimental procedures as the above authors, powder specimens were synthesized over a wide range of composition on the $LiTaO_3–CaZrO_3$ join for temperatures ranging between 1100 and 1350°C. Examination of these specimens via X-ray powder diffraction and transmission electron microscopy (TEM) gave results that were only partially in agreement with the earlier reported results—in particular a previously unreported, fluorite-related, superstructure phase was clearly present in all specimens from 45 to 90 mol% $CaZrO_3$ in addition to the wide range solid solution phase reported by Neurgaonkar *et al.* (1) and Smith and West (2).

As lithium loss appeared to be a possible explanation for our results relative to those of earlier studies, an investigation of lithium-deficient and lithium-free specimens was undertaken. This investigation showed that the new long period, fluorite-related superstructure phase was indeed lithium-free. The purpose of this paper is to present these results with a focus upon the new long period, fluorite-related superstructure phase.

2. EXPERIMENTAL

Synthesis

The starting materials used to prepare all specimens were $CaCO_3$ (Ajax Chemicals 99.0%), Li_2CO_3 (Merck), Ta_2O_5 (Atlantic Equipment Engineers 99.8%), and ZrO_2 (Z-tech). Following Smith and West (2), $CaZrO_3$ and $LiTaO_3$ were first prepared by grinding together the appropriate reagents ($CaCO_3/ZrO_2$ and Li_2CO_3/Ta_2O_5, respectively), heating at 800°C for 3 h to remove CO_2, and then firing at 1350 and 1000°C, respectively, for a further 15–20 h. Specimens nominally on the $LiTaO_3–CaZrO_3$ join were then prepared by grinding the two components together in the appropriate proportions, pressing the powder into pellets, and reacting on alumina plates in a furnace at 1100 or 1350° for periods ranging from 2–6 days depending upon composition.

As a result of our suspicion that lithium loss was playing a role, a range of lithium-deficient and lithium-free specimens were also prepared. It then became clear that the long period superstructure phase was lithium-free as a starting

[1] To whom all correspondence should be addressed.

0022-4596/96 $18.00

composition of $0.290TaO_{2.5} \cdot 0.355ZrO_2 \cdot 0.355CaO$ gave apparently single-phase material. To determine the composition range of the superstructure phase therefore required an investigation of the $Ta_2O_5–ZrO_2–CaO$ system in the vicinity of the superstructure composition. Specimens were prepared by grinding together the appropriate reagents and were fired at 1350°C for varying times. Variability in the XRD patterns suggested that the formation of the products at this temperature was slow. Specimens were therefore reground and reheated up to three times in order to achieve equilibrium.

Characterization

All specimens were studied by XRD using a Guinier–Hägg camera with Cu$K\alpha_1$ radiation (wavelength 1.54056 Å) and with Si (a = 5.43088 Å) as an internal standard. Transmission electron microscope (TEM) studies were performed on JEOL 100CX and Philips EM430 electron microscopes. Specimens were ground under *n*-butanol, and a drop of the suspension was left to evaporate on carbon coated copper grids. Energy dispersive spectroscopy (EDS) was carried out on a Philips EM430 TEM using a Si detector supported by a PV9900 analysis system. Quantitative EDS data were also collected using a JEOL 6400 scanning electron microscope (SEM). Analyses were made at 15 kV and 1 nA using a Link ATW detector (138 eV resolution), and data were processed using the Link ISIS system. ZAF corrections were made using the SEMQUANT software package. For quantification purposes, $CaZrO_3$, $Ca_2Ta_2O_7$, $Ta_2Zr_6O_{17}$, and H-Ta_2O_5 specimens were synthesized and used as standards.

3. RESULTS AND DISCUSSION

Examination of the powder patterns of specimens nominally on the $LiTaO_3–CaZrO_3$ join (at 0, 10, 30, 40, 45, 50, 55, 60, 70, 80, 90, 97, and 100 mol% $CaZrO_3$) showed, as expected, an ilmenite type $LiTaO_3$ solid solution existing between 0 and ~10 to 30 mol% $CaZrO_3$. An orthorhombic perovskite-like solid solution was present in all specimens with compositions in the range from 45 to 100 mol% $CaZrO_3$, with the corresponding lines in the powder pattern shifting systematically to higher 2θ as the nominal lithium content increased. In addition, the 90 mol% specimen showed the presence of two orthorhombic perovskite-like phases consistent with the previously reported two phase region.

Unexpectedly, however, a previously unreported, fluorite-related, superstructure phase was also observed in all specimens from 45 to 90 mol% $CaZrO_3$. The relative proportion of this superstructure phase to the $CaZrO_3$ type solid solution phase increased continuously as the concentration of $CaZrO_3$ decreased from 90 until ~55 mol% $CaZrO_3$ when the superstructure phase was the majority phase present, with the XRD lines due to the $CaZrO_3$ solid solution being barely visible. The fixed position of the superstructure lines across the whole of this composition range suggests that it is a line phase with well-defined stoichiometry. The strong subcell reflections were indexed to an *I*-centered orthorhombic cell of dimensions a_p = 3.640, b_p = 3.681, and c_p = 5.173 Å (p for parent), thus strongly suggesting an underlying fluorite-related parent structure. (Note that this *I*-centered parent unit cell $\mathbf{a}_p, \mathbf{b}_p, \mathbf{c}_p$ is equivalent to the more usual *F*-centered cell $\mathbf{a}_F = \mathbf{a}_p + \mathbf{b}_p, \mathbf{b}_F = -\mathbf{a}_p + \mathbf{b}_p, \mathbf{c}_F = \mathbf{c}_p$ of fluorite type structures.) Other weaker lines belonging to the superstructure phase were also clearly present but it was not possible to index them on the basis of XRD alone.

Individual grains of this phase were therefore investigated via transmission electron microscopy (TEM). Figure 1 shows (a) [100], (b) [010], (c) [001], and (d) ⟨031⟩ zone axis microdiffraction patterns of this phase. These electron diffraction patterns show that the true unit cell of this superstructure phase is $a \sim 36.4$, $b \sim 7.4$, and $c \sim 31.0$ Å, i.e., a $10 \times 2 \times 6$ superstructure with respect to the above parent unit cell. The refined unit cell dimensions from Guinier XRD data are a = 36.372(3), b = 7.3590(5), and c = 31.018(8) Å. In each of Figs. 1a–1d, the strong Bragg reflections (hereafter labeled $\mathbf{G}_F$) of the underlying fluorite type substructure are clearly visible. Note that $\mathbf{a}^* = \frac{1}{10}\mathbf{a}_p^* = \frac{1}{20}(-2, 2, 0)_F^*$, $\mathbf{b}^* = \frac{1}{2}\mathbf{b}_p^* = \frac{1}{4}(220)_F^*$, $\mathbf{c}^* = \frac{1}{6}\mathbf{c}_p^* = \frac{1}{12}(002)_F^*$. The observed extinction conditions imply a resultant space group symmetry of *Fddd*.

From a modulated structure point of view, the strongest satellite reflections present in Fig. 1b are of the form $\mathbf{G}_F \pm (404)^*$, i.e., $\mathbf{G}_F \pm (-0.4, 0.4, 0.666)_F^*$. Such satellite reflections also account for most of the nonparent lines visible in the Guinier films. The remainder of the satellite reflections visible in the Guinier films were reflections of the form $\mathbf{G}_F \pm (0.6, 0.4, -0.50)_F^*$, e.g., (913)* (arrowed in (d)). It is interesting to note that both these modulation wavevectors ($(-0.4, 0.4, 0.666)_F^*$ and $(0.6, 0.4, -0.50)_F^*$) fall close to $\frac{1}{2}\{111\}_F^*$ and suggest a relationship to the so-called cubic stabilized zirconias (CSZs) and other fluorite-related superstructure phases such as $CaZr_4O_9$ which also show additional scattering in similar regions of reciprocal space (3–6). Semi-quantitative analysis by energy dispersive spectroscopy (EDS) on individual grains of this superstructure phase obtained by reacting together $CaZrO_3$ and $LiTaO_3$ as described above confirmed that it contained equal amounts of Ca and Zr and ~82% as much Ta. This supported the composition $0.55CaZrO_3 \cdot 0.45LiTaO_3$, although the amount of Li present could not be determined.

In order to investigate whether Li is or is not present in the superstructure phase a range of Li-deficient and Li-free specimens centered on 55 mol% $CaZrO_3$ were prepared. Specimens with one third, two thirds, and all the Li removed (i.e., $0.55CaO \cdot 0.55ZrO_2 \cdot 0.45TaO_{2.5} \cdot 0.150$

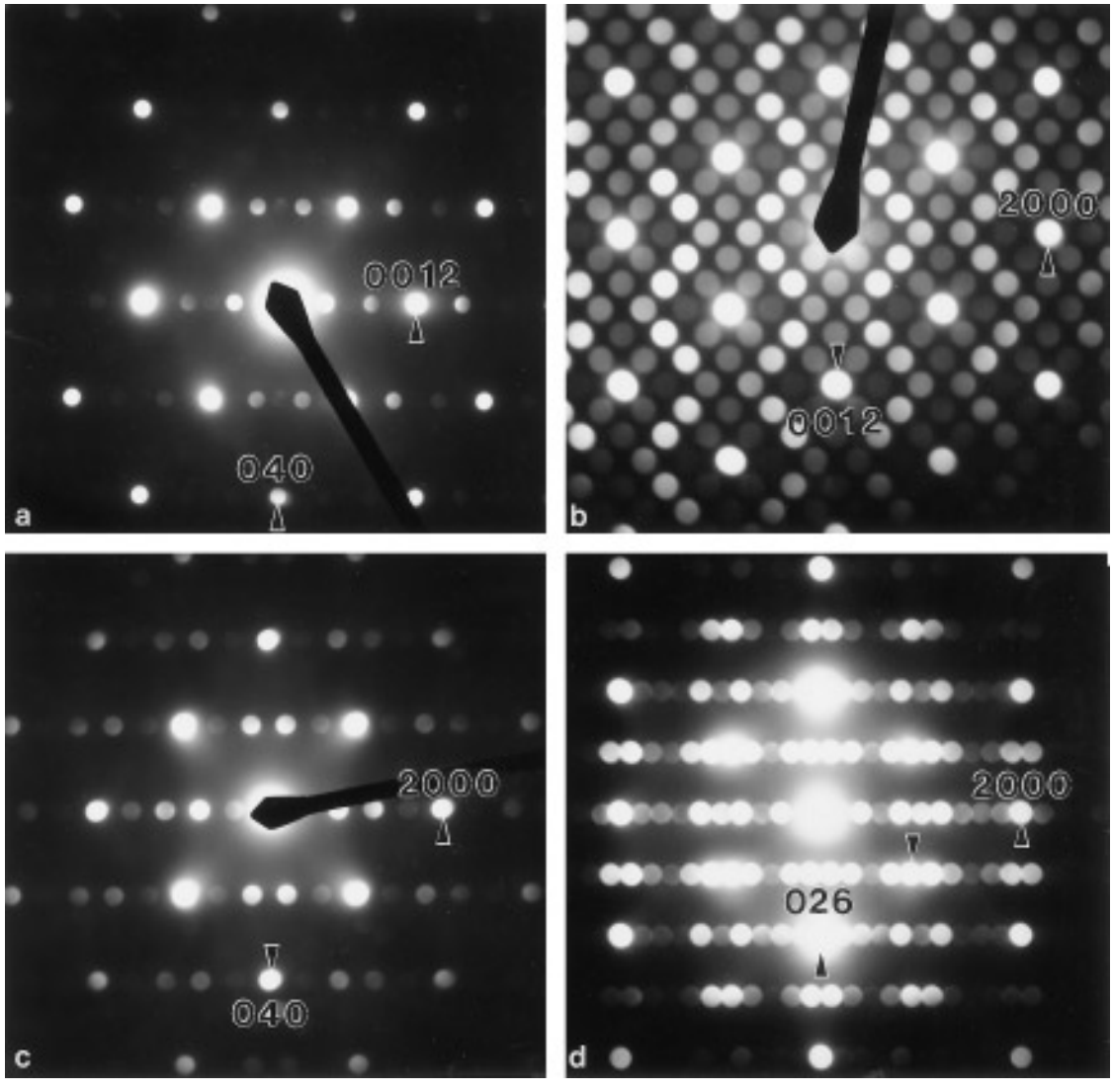

FIG. 1. Electron microdiffraction patterns of the new fluorite-related superstructure phase along the (a) [100], (b) [010], (c) [001], and (d) ⟨031⟩ zone axes.

Li_2O, $0.55CaO \cdot 0.55ZrO_2 \cdot 0.45TaO_{2.5} \cdot 0.075Li_2O$, and $0.55CaO \cdot 0.55ZrO_2 \cdot 0.45TaO_{2.5} \cdot 0.000Li_2O$) were then synthesized. XRD patterns of these specimens showed a systematic decrease in intensity of the superstructure lines combined with the appearance of a new set of lines belonging to $Ca_2Ta_2O_7$. This result appeared to show that the superstructure phase requires lithium to be present. Investigation by TEM of the specimen with no Li present, however, detected a small amount of the superstructure phase. Close reexamination of the XRD pattern of this specimen confirmed that a trace amount of the superstructure phase was present. This required the superstructure phase to be able to exist without lithium. Therefore a new Li-free specimen was synthesized. Great care was taken to ensure that the starting products were very thoroughly mixed. After a first heating, both the superstructure phase and $Ca_2Ta_2O_7$ were present. Upon regrinding and reheating, however, the $Ca_2Ta_2O_7$ lines disappeared and apparently single phase superstructure was obtained. This result was quite reproducible and would suggest a composition for the superstructure phase of $0.290TaO_{2.5} \cdot 0.355ZrO_2 \cdot 0.355CaO$. The care required to obtain equilibrium is consistent with the sluggish kinetics mentioned above and characteristic of this system.

The exact composition of this single phase material was then reexamined by EDS in both the TEM and SEM. Using $CaZrO_3$ and $Ca_2Ta_2O_7$ as standards, multiple EDS analyses in the TEM gave a superstructure composition of $0.32(1)TaO_{2.5} \cdot 0.34(1)ZrO_2 \cdot 0.34(1)CaO$ with an estimated error (based on reproducibility of analyses) in the

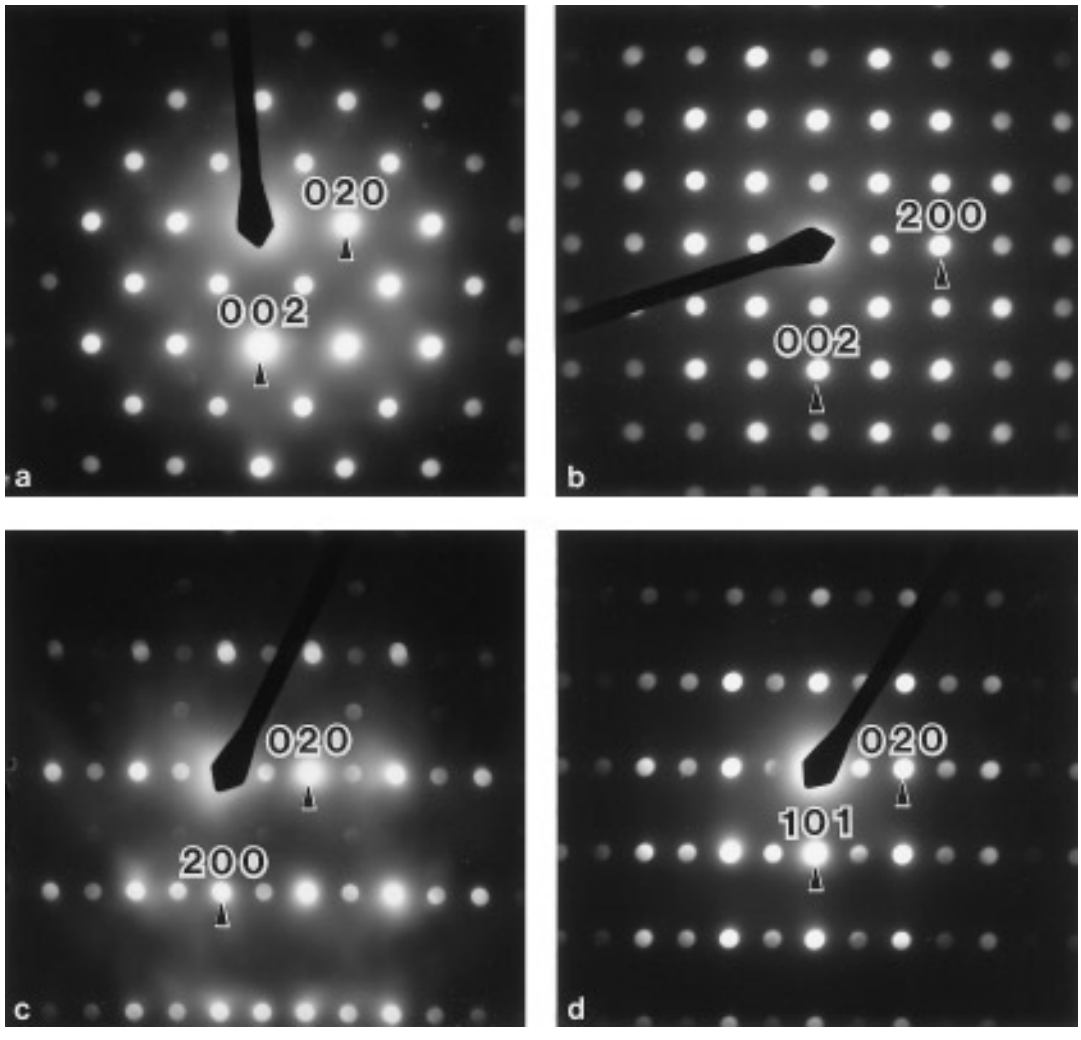

FIG. 2. Electron microdiffraction patterns of $0.227TaO_{2.5} \cdot 0.257ZrO_2 \cdot 0.516CaO$ along the (a) [100], (b) [010], (c) [001], and (d) [101] zone axes.

Ta/Ca and Ca/Zr ratios of ~5%. The most accurate results (both in terms of reproducibility and absolute accuracy) were obtained from the SEM and gave a composition of $0.304(4)TaO_{2.5} \cdot 0.347(4)ZrO_2 \cdot 0.349(4)CaO$. The accuracy of the EDS standards used was confirmed by analysis of specimens of known stoichiometry, namely $Ta_2Zr_6O_{17}$ and $CaZrO_3$. A very small amount of a ZrO_2-rich phase was also detected in the back-scattered electron image and provides a possible explanation of the slight deviation of the superstructure composition away from the $0.290TaO_{2.5} \cdot 0.355ZrO_2 \cdot 0.355CaO$ composition suggested by the original mixture of the educts.

Several Li-free specimens were also synthesized around the experimental superstructure phase composition of $0.304(4)TaO_{2.5} \cdot 0.347(4)ZrO_2 \cdot 0.349(4)CaO$ to confirm whether or not the superstructure phase was a line phase. XRD of multiphase specimens containing the superstructure phase at compositions enriched in Ta_2O_5, ZrO_2, or CaO with respect to the experimental superstructure phase composition all gave the same positions and relative intensities for the lines of the superstructure phase. These syntheses strongly support the notion that the superstructure phase is a fully ordered, anion-deficient, fluorite-related line phase. Such anion-deficient, fluorite-related phases are based on fully occupied, essentially fcc metal atom arrays with the deficiency of oxygen with respect to the ideal MO_2 stoichiometry taken up by nominally ''vacant'' anion sites (4).

The resultant cell dimensions of the superstructure phase ($10\mathbf{a}_p \times 2\mathbf{b}_p \times 6\mathbf{b}_p$) require that there be $10 \times 2 \times 6 \times 2 = 240$ metal ions per supercell. The experimentally determined composition $0.304(4)TaO_{2.5} \cdot 0.347(4)ZrO_2 \cdot 0.349(4)CaO$ requires that the number of Ca ions per supercell, n_{Ca}, equals n_{Zr} within experimental error. Hence $2n + n_{Ta} = 240$. Experimentally $n_{Ta}/n = \xi = 0.87(2)$. Hence $n(2 + \xi) = 240$. The only low order fraction within the

experimental bounds for ξ consistent with a fully ordered cation array is $\xi = \frac{6}{7} = 0.857$ and implies an overall supercell stoichiometry of $Ca_{84}Zr_{84}Ta_{72}O_{432}$ (i.e., $Ca_7Zr_7Ta_6O_{36}$) with a nominal anion vacancy concentration of $\frac{4}{40}$, i.e., 10%. Refinement of the cation and anion vacancy distributions and associated structural relaxations away from the ideal fluorite parent positions in this phase is by no means a trivial task. Unfortunately, to date, it has not proved possible to synthesize a single crystal of this phase, but work is in progress to attempt to model the superstructure using high resolution XRD data collected using a synchrotron X-ray source.

During the course of this synthetic work an orthorhombic perovskite type solid solution phase closely related to $CaZrO_3$ itself (and hence to the solid solution phases reported in (1–2)) was discovered close to the join connecting $Ca_2Ta_2O_7$ and $CaZrO_3$. A specimen of nominal composition $0.260TaO_{2.5} \cdot 0.313ZrO_2 \cdot 0.426CaO$ was prepared and found to contain a mixture of the superstructure phase and a cation-deficient, orthorhombic perovskite type phase of composition $0.227TaO_{2.5} \cdot 0.257ZrO_2 \cdot 0.516CaO$ (i.e., $Ca_{0.969}Zr_{0.483}Ta_{0.426}O_3$) as determined by quantitative analysis on the SEM (using $Ca_2Ta_2O_7$ and $CaZrO_3$ as standards).

Figure 2 shows (a) [100], (b) [010], (c) [001], and (d) [101] zone axis SADPs characteristic of this phase. The observed extinction conditions require space group symmetry of at least $Pn2_1a$ but most probably *Pnma*, as for $CaZrO_3$ itself. The similarity of the powder patterns leaves no doubt that this phase and $CaZrO_3$ itself are very closely related. Measurement of the corresponding Guinier film showed that the lines belonging to this phase had moved quite substantially with respect to the corresponding lines in the end-member $CaZrO_3$. It is thus clear that substantial amounts of $TaO_{2.5}$ can be incorporated into $CaZrO_3$ regardless of whether or not Li is present.

Two specimens ($0.38Ca_2Ta_2O_7 \cdot 0.62CaZrO_3$ and $0.15Ca_2Ta_2O_7 \cdot O.85CaZrO_3$) were then prepared on the join connecting this composition with $CaZrO_3$ in an attempt to investigate the composition range of existence of this solid solution. The lines in the latter, apparently single phase, specimen again belonged to the orthorhombic perovskite type phase suggesting the existence of a wide range solid solution. Electron diffraction patterns were identical to those shown in Fig. 2. The measured unit cell dimensions for this composition were $a = 5.708(1)$, $b = 7.976(3)$, and $c = 5.571(2)$ Å. The former specimen, however, was multiphase and contained lines belonging to the superstructure phase as well as to the phase of orthorhombic perovskite type.

A range of further specimens were synthesized both on and off the join connecting $Ca_2Ta_2O_7$ and $CaZrO_3$. Despite repeated regrindings and reheatings, however, many of these specimens were clearly nonequilibrium presumably as a result of the extremely sluggish kinetics of this system. This precluded determination of the full extent of the solid solution.

While it has not proved experimentally possible to determine the extent of the solid solution phase based on $CaZrO_3$ in the $CaO–ZrO_2–Ta_2O_5$ system there is no doubt that substantial amounts of Ta_2O_5 can be incorporated into $CaZrO_3$. The relationship of this solid solution to the previously reported $CaZrO_3$ type solid solutions in the $LiTaO_3–CaZrO_3$ system remains to be determined. It may be significant that the measured unit cell dimensions for $0.15Ca_2Ta_2O_7 \cdot 0.85CaZrO_3$ correspond to those reported for ~83 mol% $CaZrO_3$ in (2). Further consideration, however, is beyond the scope of the current paper.

REFERENCES

1. R. R. Neurgaonkar, T. C. Lim, and E. J. Staples, *Mater. Res. Bull.* **13,** 635 (1978).
2. R. I. Smith and A. R. West, *J. Solid State Chem.* **108,** 29 (1994).
3. J. G. Allpress and H. J. Rossell, *J. Solid State Chem.* **15,** 68 (1975).
4. H. J. Rossell, J. R. Sellar, and I. J. Wilson, *Acta Crystallogr. Sect. B* **47,** 862 (1991).
5. R. Miida, M. Tanaka, H. Arashi, and M. Ishigame, *J. Appl. Crystallogr.* **27,** 67 (1994).
6. T. R. Welberry, R. L. Withers, and S. C. Mayo, *J. Solid State Chem.* **115,** 43 (1995).